TECHNICAL RESEARCH REPORT

Instability Monitoring and Control of Power Systems

by Eyad H. Abed, Munther A. Hassouneh, Mohamed S. Saad

TR 2004-36

ISR develops, applies and teaches advanced methodologies of design and analysis to solve complex, hierarchical, heterogeneous and dynamic problems of engineering technology and systems for industry and government.

ISR is a permanent institute of the University of Maryland, within the Glenn L. Martin Institute of Technology/A. James Clark School of Engineering. It is a National Science Foundation Engineering Research Center.

Web site http://www.isr.umd.edu

INSTABILITY MONITORING AND CONTROL OF POWER SYSTEMS

Eyad H. Abed, Munther A. Hassouneh and Mohamed S. Saad
Department of Electrical and Computer Engineering and
the Institute for Systems Research
University of Maryland, College Park, MD 20742, USA
abed@umd.edu, munther@umd.edu, mssaad@umd.edu

Abstract Today's electric power systems are often subject to stress by heavy loading conditions, resulting in operation with a small margin of stability. This has led to research on estimating the distance to instability. Most of these research efforts are solely model-based. In this work, a signal-based approach for real-time detection of impending instability is considered. The main idea pursued here involves using a small additive white Gaussian noise as a probe signal and monitoring the spectral density of one or more measured states for certain signatures of impending instability. Input-to-state participation factors are introduced as a tool to aid in selection of locations for probe inputs and outputs to be monitored. Since these participation factors are model-based, the chapter combines signal-based and model-based ideas toward achieving a robust methodology for instability monitoring.

Keywords: Monitoring, power systems, stability, instability, precursors, bifurcation, voltage collapse, participation factors.

1. Introduction

Today's electric power systems are often subject to stress due to heavy loading conditions. Under such conditions, a power system that appears to be functioning well could actually be very vulnerable to loss of stability. Stability loss can, in turn, trigger a chain of events leading to failure of the system. Stability loss can occur in several forms, but the most common one resulting from heavy load conditions is voltage instability, which leads to voltage collapse through cascading of system events [11]. This differs markedly from transient instability following a system contingency, since this type of instability usually results from slow changes

in system parameters, such as loading or generation. There is an inherent difficulty in predicting voltage instability, since the parameter values at which it occurs depend on component dynamics in an uncertain and complex interconnected system. Inaccurate system models can easily yield incorrect results for the stability envelope of the system. When a system must be operated near its stability limits, any model uncertainty can result in the system exiting its stable operating regime without warning. Even the most detailed calculations are insufficient in these circumstances.

In this chapter, instability monitoring using (noisy) probe signals is considered. The use of probe signals is shown to help reveal an impending loss of stability. This is because probe signals propagate in the power system and give certain signatures near an instability that can be used as a warning signals for possible impending voltage collapse. Such warning signals are needed to alert system operators of a situation that may require preventive control, and to provide the operators with valuable additional time to take necessary preventive (rather than corrective) measures.

The chapter proceeds as follows. In Section 2, participation factors for linear systems are discussed. This includes both the modal participation factors, and newly introduced input-to-state participation factors. In Section 3, a signal-based approach to instability monitoring is presented. In Section 4, three case studies are given that demonstrate the proposed approach to instability monitoring. Concluding remarks are collected in Section 5.

2. Participation Factors

As mentioned above, the approach to instability monitoring presented in this chapter involves injecting probe signals at certain locations in a power network and monitoring the effects on measured output variables. Participation factors, specifically input-to-state participation factors introduced in this section, play an important role in selection of sites for probe signal injection and output measurement. Because of this, a brief summary of modal participation factors is given first, along with a derivation of input-to-state modal participation factors. This will be helpful background in the discussion of precursor-based monitoring in the next section.

Participation factors are nondimensional scalars that measure the interaction between the modes and the state variables of a linear system [9, 12, 2]. Since their introduction in [9, 12], participation factors

have been used for analysis, order reduction and controller design in a variety of fields, especially electric power systems.[1]

2.1 Modal participation factors

Consider a general continuous-time linear time-invariant system

$$\dot{x} = Ax(t) \tag{1.1}$$

where $x \in \Re^n$, and A is a real $n \times n$ matrix. Suppose that A has a set of n distinct eigenvalues $(\lambda_1, \lambda_2, \ldots, \lambda_n)$. Let $(r^1, r^2, \ldots, r^n)$ be right eigenvectors of the matrix A associated with the eigenvalues $(\lambda_1, \lambda_2, \ldots, \lambda_n)$, respectively. Let $(l^1, l^2, \ldots, l^n)$ denote left (row) eigenvectors of the matrix A associated with the eigenvalues $(\lambda_1, \lambda_2, \ldots, \lambda_n)$, respectively.

The right and left eigenvectors are taken to satisfy the normalization

$$l^i r^j = \delta_{ij}$$

where δ_{ij} is the Kronecker delta:

$$\delta_{ij} = \begin{cases} 1 & i = j \\ 0 & i \neq j \end{cases}$$

The definition of modal participation factors is as follows. The participation factor of the i-th mode in the k-th state is defined to be the complex number

$$p_{ki} := l_k^i r_k^i$$

This formula also gives the participation of the k-th state in the i-th mode. Participation factors measure the level of participation of modes in states and the level of participation of states in modes. The participation factors are dimensionless quantities that are independent of the units in which state variables are measured [9, 12, 2].

2.2 Input-to-state participation factors

The concept of participation factors of modes in states and vice versa has been extended to linear time invariant systems with inputs [16]

$$\dot{x} = Ax + Bu \tag{1.2}$$
$$y = Cx. \tag{1.3}$$

We consider the case where the input is applied to one component, say the q-th component, of the right side of (1.2) and only one state, say the

k-th state, is measured. That is, in Eqs. (1.2)-(1.3), B and C take the form

$$\begin{aligned} B = e^q = [0 \ \dots \ 0 \ \underbrace{1}_{q-th} \ 0 \dots 0]^T, \\ C = (e^k)^T = [0 \ \dots \ 0 \ \underbrace{1}_{k-th} \ 0 \dots 0]. \end{aligned} \tag{1.4}$$

With this choice of C and B, in steady state the output in (1.3) (in the frequency domain) is given by

$$\begin{aligned} y(s) = x_k(s) &= C(sI - A)^{-1}Bu \\ &= \sum_{i=1}^{n} \frac{Cr^i l^i B}{s - \lambda_i} u(s) \\ &= \sum_{i=1}^{n} \frac{r_k^i l_q^i}{s - \lambda_i} u(s) \end{aligned} \tag{1.5}$$

We take

$$\begin{aligned} p_{qk}^i &= |Cr^i l^i B| \\ &= |r_k^i l_q^i| \end{aligned} \tag{1.6}$$

as *the participation factor of mode i in state k when the input is applied to state q*. We call this quantity the *input-to-state participation factor (ISPF)* for mode i, with measurement at state k and input applied to state q. Note that the ISPF is dimensionless given that the input and output vectors B and C take the special form in (1.4). In [8], the quantity $p_{qk}^i = r_k^i l_q^i$ is called a generalized participation.

3. Precursor-Based Monitoring

As noted by Hauer [5], the recurring problems of system oscillations and voltage collapse are due in part to system behavior not well captured by the models used in planning and operation studies. In the face of component failures, system models quickly become mismatched to the physical network, and are only accurate if they are updated using a powerful and accurate failure detection system. Therefore, it is important to employ nonparametric techniques for instability monitoring. In this work, noisy probe signals are used to help detect impending loss of stability.

Recently, Kim and Abed [7] developed monitoring systems for detecting impending instability in nonlinear systems. The work builds on Wiesenfeld's research on "noisy precursors of bifurcations," which were

originally introduced to characterize and employ the noise amplification properties of nonlinear systems near various types of bifurcations [14, 15]. Noisy precursors are features of the power spectral density (PSD) of a measured output of a system excited by additive white Gaussian noise (AWGN). In [7], the noisy precursors concept was extended from systems operating at limit cycles to systems operating near equilibria, and closed-loop monitoring systems were developed to facilitate use of noisy precursors in revealing impending loss of stability for such systems. It was shown in [7] that systems driven by white noise and operating near an equilibrium point exhibit sharply growing peaks near certain frequencies as the system nears a bifurcation. In particular, it was shown that for stationary bifurcation where an eigenvalue passes through the origin (as in the case of pitchfork or transcritical bifurcation), the peak in the PSD occurs at zero frequency. Analogously, for the case of Hopf bifurcation (complex conjugate pair of eigenvalues crossing the imaginary axis transversely), the peak in the PSD occurs near ω_c, the critical frequency of the Hopf bifurcation.

In this work, we show that noisy precursors can be used as a warning signal indicating that the power system is operating dangerously close to instability. We also show that the spectrum of a measured state of the system is proportional to the square of the input-to-state participation factors. Thus, ISPFs can be used to determine the best location for applying the probe signal and for choosing which state to measure where the noisy precursor would be most apparent. Figure 1.1 shows a schematic diagram of our instability monitoring technique.

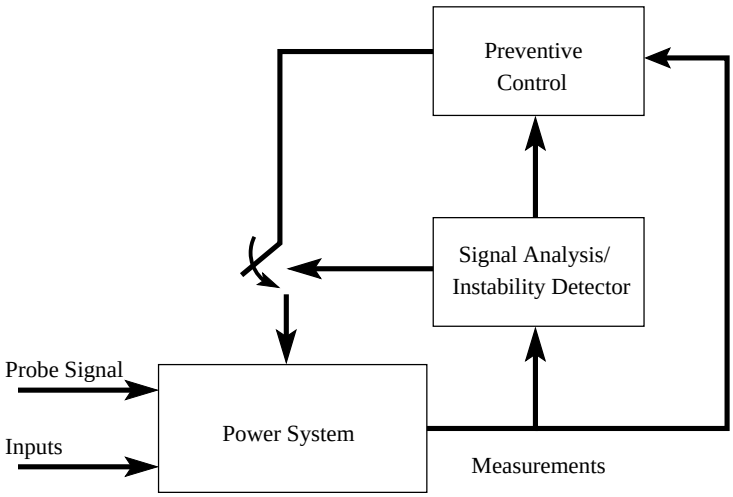

Figure 1.1. Precursor-based instability monitor with external probe signal.

Consider a nonlinear dynamic system ("the plant")

$$\dot{x} = f(x, \mu) + \xi(t) \tag{1.7}$$

where $x \in R^n$, μ is a bifurcation parameter, and $\xi(t) \in R^n$ is a zero-mean vector white Gaussian noise process [7]. Let the system possess an equilibrium point x_0. For small perturbations and noise, the dynamical behavior of the system can be described by the linearized system in the vicinity of the equilibrium point x_0. The linearized system corresponding to (1.7) with a small noise forcing $\xi(t)$ is given by

$$\dot{x} = Df(x_0, \mu)x + \xi(t) \tag{1.8}$$

where x now denotes $x - x_0$ (the state vector referred to x_0). For the results of the linearized analysis to have any bearing on the original nonlinear model, we must assume that the noise is of small amplitude.

The noise $\xi(t)$ can occur naturally or can be injected using available controls. We consider the case where the noise is applied to one state and the power spectral density of another state is calculated. That is, we consider the case where $\xi(t) = B\eta(t)$ with $B = e^q = [0 \ \dots \ 0 \ \underbrace{1}_{q-th} \ 0 \dots 0]^T$, $\eta(t)$ is a scalar white Gaussian noise with zero mean and power σ^2, and the output is given by $y = Cx$ with $C = (e^p)^T = [0 \ \dots \ 0 \ \underbrace{1}_{p-th} \ 0 \dots 0]$.

In steady state, the output of system (1.8) forced by a small AWGN is given by

$$\begin{aligned} y(s) = x_p(s) &= \sum_{i=1}^{n} \frac{Cr^i l^i B}{s - \lambda_i} \eta(s) \\ &= \sum_{i=1}^{n} \frac{r_p^i l_q^i}{s - \lambda_i} \eta(s). \end{aligned} \tag{1.9}$$

The power spectral density of the output of a linear system with transfer function $H(j\omega)$ is related to the power spectral density of the input by [6]

$$S_y(\omega) = H(j\omega)H(-j\omega)S_\eta(\omega) \tag{1.10}$$

Thus, the power spectrum of the p-th state is given by

$$\begin{aligned} S_{x_p} &= \left(\sum_{i=1}^{n} \frac{r_p^i l_q^i}{j\omega - \lambda_i} \right) \left(\sum_{k=1}^{n} \frac{r_p^k l_q^k}{-j\omega - \lambda_k} \right) \sigma^2 \\ &= \sigma^2 \sum_{i=1}^{n} \sum_{k=1}^{n} \frac{r_p^i l_q^i}{j\omega - \lambda_i} \ \frac{r_p^k l_q^k}{-j\omega - \lambda_k} \end{aligned} \tag{1.11}$$

Suppose that the system is nearing a Hopf bifurcation. Specifically, assume that a complex conjugate pair of eigenvalues is close to the imaginary axis, and has relatively small negative real part in absolute value compared to other system eigenvalues. Denote this pair as $\lambda_{1,2} = -\epsilon \pm j\omega_c$, with $\epsilon > 0$ small and $\omega_c > 0$:

$$|Re(\lambda_i)| \gg \epsilon, \quad i = 3, \ldots, n. \tag{1.12}$$

Under this assumption, $S_{x_p}(\omega)$ can be approximated as

$$\begin{aligned}
S_{x_p}(\omega) &\approx \sigma^2 \sum_{i=1}^{2}\sum_{k=1}^{2} \frac{r_p^i l_q^i}{j\omega - \lambda_i} \; \frac{r_p^k l_q^k}{-j\omega - \lambda_k} \\
&= \sigma^2 \left(\frac{1}{\epsilon + j(\omega - \omega_c)} \; \frac{1}{\epsilon - j(\omega + \omega_c)} (r_p^1 l_q^1)^2 \right. \\
&+ \frac{1}{\epsilon + j(\omega + \omega_c)} \; \frac{1}{\epsilon - j(\omega - \omega_c)} (r_p^2 l_q^2)^2 \\
&+ \frac{1}{\epsilon + j(\omega - \omega_c)} \; \frac{1}{\epsilon - j(\omega - \omega_c)} r_p^1 l_q^1 r_p^2 l_q^2 \\
&+ \left. \frac{1}{\epsilon + j(\omega + \omega_c)} \; \frac{1}{\epsilon - j(\omega + \omega_c)} r_p^1 l_q^1 r_p^2 l_q^2 \right) \\
&= \sigma^2 \left(\frac{|r_p^1 l_q^1|^2}{\epsilon^2 + (\omega - \omega_c)^2} + \frac{|r_p^1 l_q^1|^2}{\epsilon^2 + (\omega + \omega_c)^2} \right. \\
&+ \left. 2\mathrm{Re}\left\{ \frac{1}{\epsilon + j(\omega - \omega_c)} \; \frac{1}{\epsilon - j(\omega + \omega_c)} (r_p^1 l_q^1)^2 \right\} \right). \qquad (1.13)
\end{aligned}$$

Here, r_p^i denotes the p-th component of the i-th right eigenvector r^i (the eigenvector corresponding to λ_i), and l_q^i denotes the q-th component of the i-th left eigenvector l^i. Note that all terms containing λ_i, $i = 3, \ldots, n$ have been neglected and only terms containing the critical eigenvalues λ_1 and λ_2 have been retained. After algebraic manipulation and substituting $(r_p^1 l_q^1)^2 = \alpha + j\beta$ where $\alpha = |r_p^1 l_q^1|^2 \cos(2\theta_{pq})$ and $\beta = |r_p^1 l_q^1|^2 \sin(2\theta_{pq})$, with $\theta_{pq} = \tan^{-1}\left(\frac{Im\{r_p^1 l_q^1\}}{Re\{r_p^1 l_q^1\}}\right)$, the power spectral density of x_p can be rewritten as

$$\begin{aligned}
S_{x_p}(\omega) &= \sigma^2 |r_p^1 l_q^1|^2 \left(\frac{1}{\epsilon^2 + (\omega - \omega_c)^2} + \frac{1}{\epsilon^2 + (\omega + \omega_c)^2} \right) \\
&+ \sigma^2 \frac{(\beta\epsilon + \alpha\omega_c)(\omega - \omega_c) + \epsilon(\epsilon\alpha - \omega_c\beta)}{(\epsilon^2 + \omega_c^2)(\epsilon^2 + (\omega - \omega_c)^2)} \\
&- \sigma^2 \frac{(\beta\epsilon + \alpha\omega_c)(\omega + \omega_c) - \epsilon(\epsilon\alpha - \omega_c\beta)}{(\epsilon^2 + \omega_c^2)(\epsilon^2 + (\omega + \omega_c)^2)}
\end{aligned}$$

$$= \sigma^2 |r_p^1 l_q^1|^2 \left[(1 + G_1(\omega)) \frac{1}{\epsilon^2 + (\omega - \omega_c)^2} + (1 - G_2(\omega)) \frac{1}{\epsilon^2 + (\omega + \omega_c)^2} \right] \quad (1.14)$$

where

$$G_1(\omega) = \frac{(\epsilon \sin(2\theta_{pq}) + \omega_c \cos(2\theta_{pq}))(\omega - \omega_c) + \epsilon(\epsilon \cos(2\theta_{pq}) - \omega_c \sin(2\theta_{pq}))}{\epsilon^2 + \omega_c^2},$$

$$G_2(\omega) = \frac{(\epsilon \sin(2\theta_{pq}) + \omega_c \cos(2\theta_{pq}))(\omega + \omega_c) - \epsilon(\epsilon \cos(2\theta_{pq}) - \omega_c \sin(2\theta_{pq}))}{\epsilon^2 + \omega_c^2}.$$

For $\omega = \omega_c$ and sufficiently small ϵ ($\epsilon \ll \omega_c$), the power spectral density of x_p is given by

$$S_{x_p}(\omega) = \sigma^2 |r_p^1 l_q^1|^2 \left(\frac{1}{\epsilon^2} + O\left(\frac{1}{\epsilon}\right) + O(1) \right). \quad (1.15)$$

Note that the ISPFs are related to the spectral densities of the states of a system driven by small AWGN as in Eq. (1.14). The amplitude of the spectrum is proportional to the square of the ISPFs. The input-to-state participation factors can be used to determine the best location for applying the probe signal and also the state that will have the highest spectral peak.

4. Case Studies

Below, the instability monitoring technique presented above is demonstrated on sample power system models. First, a single generator with dynamic load is considered. Then, a single generator with an infinite bus together with excitation control is considered. Finally, a three-generator nine-bus power system model is considered.

4.1 Single generator with dynamic load

Consider the single generator power system model with induction motor load [13]:

$$\dot{\delta_m} = \omega \quad (1.16)$$

$$M\dot{\omega} = -d_m\omega + P_m - E_m V Y_m \sin(\delta_m - \delta) \quad (1.17)$$

$$K_{qw}\dot{\delta} = -K_{qv2}V^2 - K_{qv}V + Q(\delta_m, \delta, V) - Q_0 - Q_1 \quad (1.18)$$

$$TK_{q\omega}K_{pv}\dot{V} = K_{p\omega}K_{qv2}V^2 + (K_{p\omega}K_{pv} - K_{q\omega}K_{pv})V + K_{q\omega}(P(\delta_m, \delta, V) - P_0 - P_1) - K_{p\omega}(Q(\delta_m, \delta, V) - Q_0 - Q_1) \quad (1.19)$$

The state variables are δ_m (the generator phase angle, closely related to the mechanical angle of the generator rotor), ω (the rotor speed), δ (the load voltage phase angle) and V (the magnitude of the load voltage). The load includes a constant PQ load in parallel with an induction motor. The real and reactive powers supplied to the load by the network are

$$\begin{aligned} P(\delta_m, \delta, V) &= -E_0^{'} V Y_0^{'} \sin(\delta) + E_m V Y_m \sin(\delta_m - \delta), \\ Q(\delta_m, \delta, V) &= E_0^{'} V Y_0^{'} \cos(\delta) + E_m V Y_m \cos(\delta_m - \delta) \\ &- (Y_0^{'} + Y_m) V^2 \end{aligned}$$

where

$$\begin{aligned} E_0^{'} &= \frac{E_0}{\sqrt{1 + C^2 Y_0^{-2} - 2C Y_0^{-1} \cos\theta_0}} \\ Y_0^{'} &= Y_0 \sqrt{1 + C^2 Y_0^{-2} - 2C Y_0^{-1} \cos\theta_0} \\ \theta_0^{'} &= \theta_0 + \tan^{-1}\left\{ \frac{C Y_0^{-1} \sin\theta_0}{1 - C Y_0^{-1} \cos\theta_0} \right\} \end{aligned}$$

The values of the parameters for this model are given in the appendix.

It has been shown that a supercritical Hopf bifurcation occurs in this power system model as the reactive load Q_1 is increased through the critical value $Q_1^* = 2.980138$ [13].

Next, we consider the system operating at loads close to the Hopf bifurcation, say at $Q_1 = 2.9$. The corresponding operating point is $x_0 = [0.2473,\ 0,\ 0.0398,\ 0.9248]$. The Jacobian of the system at this operating point is

$$A = \begin{bmatrix} 0 & 1 & 0 & 0 \\ -324.5254 & -3.4153 & 324.5254 & -73.8611 \\ 33.3333 & 0 & -29.2479 & 72.7220 \\ -3.3656 & 0 & 1.5180 & -11.1529 \end{bmatrix}$$

The eigenvalues of A are $\{-0.7923 \pm j6.6318,\ -21.1157 \pm j10.9959\}$.

To monitor the system, an AWGN probe signal is applied to the mechanical power P_m. Figure 1.2 depicts the spectral densities for the four states δ_m, ω, δ and V for $Q_1 = 2.9$ and $\sigma = 0.001$. As it is clear from this figure, the state ω has a higher peak than all other states. Figure 1.3 demonstrates the variation of the spectral density peak near $\omega = \omega_c \approx 6.6$ rad/s as a function of the bifurcation parameter Q_1. The values of the input-to-state participation factors of the critical mode in

all states are given in Table 1.1. As predicted by the analysis in Section 3, the ordering of the peaks of the spectral densities of all states at ω_c can be predicted from the values of the ISPFs.

Table 1.1. Input-to-state participation factors and spectral peaks at ω_c.

States	Spectral peak at $\omega_c \approx 6.6318$	Input-to-state participation factors (ISPFs)
δ_m	9.528×10^{-4}	$p_{21}^1 = 2.8992$
ω	40.38×10^{-4}	$p_{22}^1 = 19.364$
δ	6.616×10^{-4}	$p_{23}^1 = 2.4013$
V	0.305×10^{-4}	$p_{24}^1 = 0.4981$

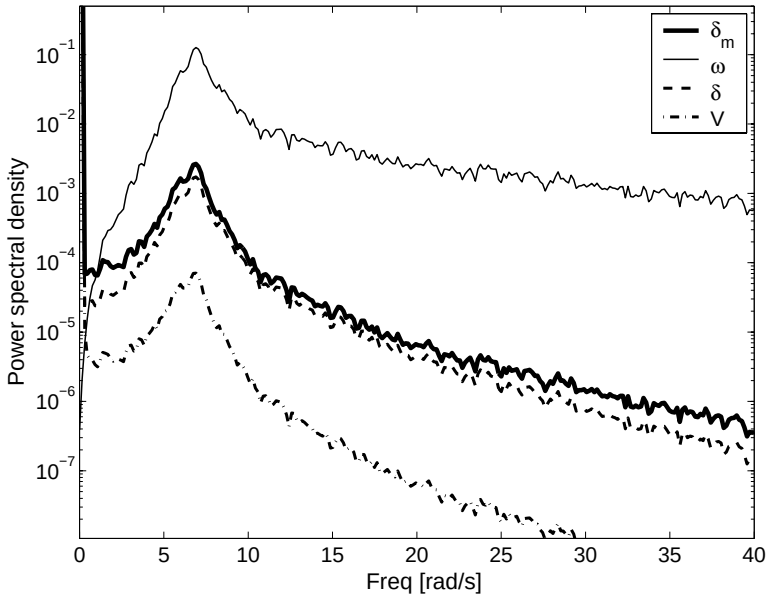

Figure 1.2. Power spectral densities of the states of the model given in (1.16)-(1.19). The bifurcation parameter was set to $Q_1 = 2.9$. White Gaussian noise of zero mean and $(0.001)^2$ power was added to P_m.

4.2 Single generator connected to an infinite bus

Consider a synchronous machine connected to an infinite bus together with excitation control [1]. It was shown [1] that this system undergoes a Hopf bifurcation as the control gain in the excitation system is increased beyond a critical value. The dynamics of the generator is given by:

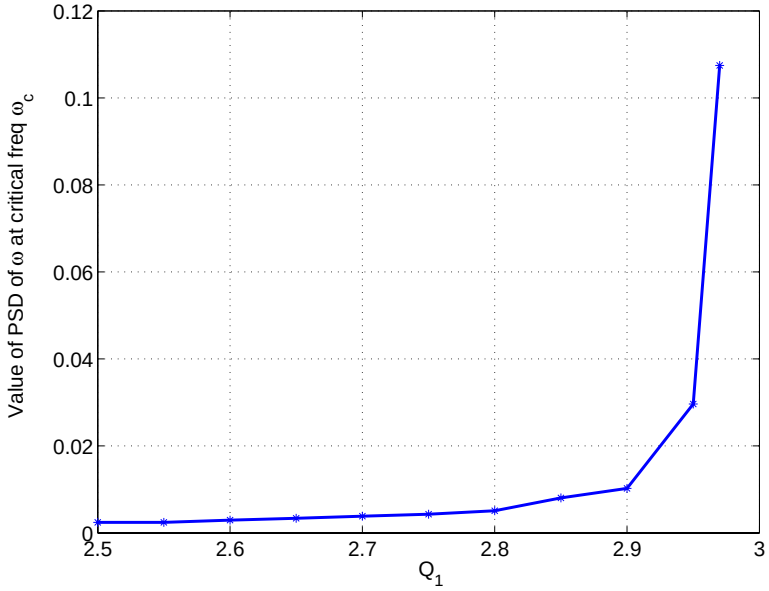

Figure 1.3. Variation of the peak value of the power spectral density of ω as a function of the bifurcation parameter Q_1. White Gaussian noise of zero mean and $(0.001)^2$ power was added to P_m.

$$\dot{\delta} = \omega \tag{1.20}$$
$$2H\dot{\omega} = -D\omega + \omega_0(P_m - P_e) \tag{1.21}$$
$$\tau'_{d0}\dot{E}'_q = E_{FD} - E'_q - (X_d - X'_d)i_d \tag{1.22}$$

with the following algebraic equations:

$$\begin{aligned}
P_e &= E_q i_q \\
E_q &= E'_q + (X_q - X'_d)i_d \\
i_d &= x(E_q - E\cos\delta) - rE\sin\delta \\
i_q &= r(E_q - E\cos\delta) + xE\sin\delta \\
x &= \frac{X_l + X_q}{R_l^2 + (X_l + X_q)^2} \\
r &= \frac{R_l}{R_l^2 + (X_l + X_q)^2}
\end{aligned}$$

The subscripts d and q refer to the direct and quadrature axes, respectively. The dynamics of the excitation control is given by

$$\tau_E\dot{E}_{FD} = -K_E E_{FD} + V_R - E_{FD}S_E(E_{FD}) \tag{1.23}$$
$$\tau_F\dot{V}_3 = -V_3 + \frac{K_F}{\tau_E}(-K_E E_{FD} + V_R - E_{FD}S_E(E_{FD})) \tag{1.24}$$
$$\tau_A\dot{V}_R = -V_R + K_A(V_{REF} - V_t - V_3) \tag{1.25}$$

Here V_t is the terminal voltage and is given by

$$V_t^2 = v_d^2 + v_q^2$$

where

$$-v_d = \psi_q = -X_q i_q$$
$$v_q = \psi_d = E'_q - X'_d i_d.$$

The saturation function $S_E(E_{FD})$ is usually approximated as $S_E(E_{FD}) = A_{EX} \exp(B_{EX} E_{FD})$. An equilibrium point of this system is denoted by $x^0 = (\delta^0, \omega^0, {E'_q}^0, E^0_{FD}, V^0_3, V^0_R)$. The values of the parameters that appear in this power system model are given in Table 1.A.1.

For $P_m = 0.937$, $V_{REF} = 1.130$, $\lambda = 2$, it has been shown that a subcritical Hopf bifurcation occurs at $K^*_A = 193.74$ [1].

Next, we consider the system operating before the Hopf bifurcation, say at $K_A = 185$. The corresponding operating point is given by $x^0 = [1.3515,\ 0,\ 1.1039,\ 2.3150,\ 0,\ 0.5472]$. The Jacobian of the system at this operating point is

$$A = \begin{bmatrix} 0 & 1 & 0 & 0 & 0 & 0 \\ -62.2 & -0.2 & -79.7 & 0 & 0 & 0 \\ -0.2 & 0 & -0.4 & 0.2 & 0 & 0 \\ 0 & 0 & 0 & -1.1 & 0 & 2 \\ 0 & 0 & 0 & 0 & -1.7 & 0.1 \\ 125.9 & 0 & -1157.6 & 0 & -1850 & -10 \end{bmatrix}.$$

The eigenvalues of A are $\{-0.0139 \pm j7.7707,\ -4.5832 \pm j12.6178, -2.1029 \pm j0.9417\}$.

Note that for this model, there are two physically feasible locations for applying the probe signal. The probe signal can be either applied to V_{ref} or to P_m. The input-to-state participation factors are used to determine the best location for applying the probe signal. From the values of the ISPFs (see Table 1.2), it is clear that mode 1 has higher participation in other states when the probe signal is applied to P_m than when applied to V_{ref}. This can be also seen from the power spectral densities shown in Figures 1.4 and 1.5. Also, the ISPFs give an indication of which state to monitor. The higher the participation factor of the critical mode in a state, the higher the peak of the spectrum for that state. Figure 1.6 shows the variation of the power spectral peak at the critical frequency as a function of the bifurcation parameter when noise is added to P_m.

4.3 Three-generator nine-bus power system

Below, we consider the Western System Coordinating Council (WSCC) 3-machine, 9-bus power system model, which is widely used in the liter-

Table 1.2. Input-to-state participation factors and spectral peaks at ω_c for the single generator connected to an infinite bus.

State	Spect. peak at $\omega \approx 7.8$ (noise added to P_m)	ISPFs	Spect. peak at $\omega \approx 7.8$ (noise added to V_{ref})	ISPFs
δ	0.0226	$p^1_{21} = 0.0648$	0.0019	$p^1_{61} = 0.0024$
ω	1.2880	$p^1_{22} = 0.4923$	0.1084	$p^1_{62} = 0.0185$
E'_q	0.75938×10^{-4}	$p^1_{23} = 0.0038$	0.68651×10^{-5}	$p^1_{63} = 0.0001$
E_{FD}	0.2326	$p^1_{24} = 0.2084$	0.0210	$p^1_{64} = 0.0078$
V_3	2.4644×10^{-4}	$p^1_{25} = 0.0068$	2.2288×10^{-5}	$p^1_{65} = 0.0003$
V_R	3.3923	$p^1_{26} = 0.8006$	0.3064	$p^1_{66} = 0.0301$

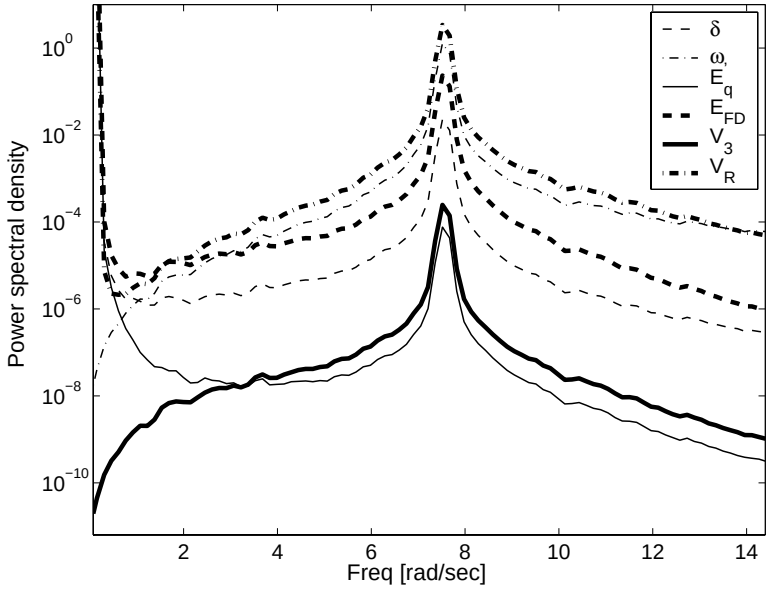

Figure 1.4. Power spectral densities of the states of the single generator connected to an infinite bus system. The bifurcation parameter was set to $K_A = 185$. White Gaussian noise of zero mean and $(0.000032)^2$ power was added to P_m.

ature [10, pp. 170–177],[3]. The dynamics of this model includes three identical IEEE-Type I exciters for the three machines. The machine data and the exciter data are given in [10, 3].

In this model, a subcritical Hopf bifurcation occurs as the load on bus 5 is increased beyond 4.5 pu [10]. Our goal in this case study is to detect this impending loss of stability by using an AWGN probe signal and continuously monitoring the power spectral densities of certain states. This would give the system operator (or an automatic controller) valuable time to take appropriate preventive measures (e.g., shedding loads

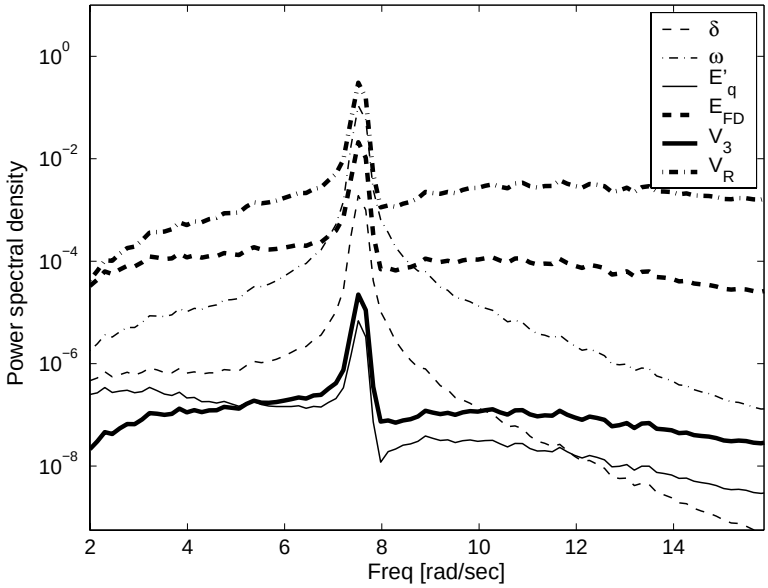

Figure 1.5. Power spectral densities of the states of the single generator connected to an infinite bus system. The bifurcation parameter was set to $K_A = 185$. White Gaussian noise of zero mean and $(0.000032)^2$ power was added to V_{ref}.

at certain buses). The simulations of this model were conducted using PSAT [3]. For values of the load on bus 5 close to 4.0 pu, the linearization of the system at the operating point has two complex conjugate pair of eigenvalues close to the imaginary axis, $\lambda_{1,2} = -0.17665 \pm j8.184$ and $\lambda_{3,4} = -0.3134 \pm j1.7197$. As the load on bus 5 is increased further, the pair $\lambda_{3,4}$ approaches the imaginary axis, while the other pair $\lambda_{1,2}$ changes only slightly. For example, when the load at bus 5 is 4.4 pu, $\lambda_{1,2} = -0.18231 \pm j8.0978$ and $\lambda_{3,4} = -0.04602 \pm j2.1151$. Increasing the load on bus 5 beyond 4.5 pu causes the pair $\lambda_{3,4}$ to cross the imaginary axis from left to right.

From the values of the ISPFs calculated for this system, we found that both of the critical modes have higher participation when the probe signal is applied to P_{m_3}, the mechanical power of generator number 3. Also, we found that these modes have high participation in the field voltage of the exciters. Therefore, in the following simulations, the probe signal is added to P_{m_3} and the power spectral densities of the field voltages of the three exciters (i.e., $E_{fd_i}, i = 1, 2, 3$) are monitored. Figure 1.7 and Figure 1.8 show the power spectral densities of E_{fd_i}, $i = 1, 2, 3$ when the load on bus 5 (P_{L_5}) is 4.0 pu and 4.4 pu, respectively. It is clear from Figure 1.7 that when the load on bus 5 is 4.0 pu, the spectrum has two

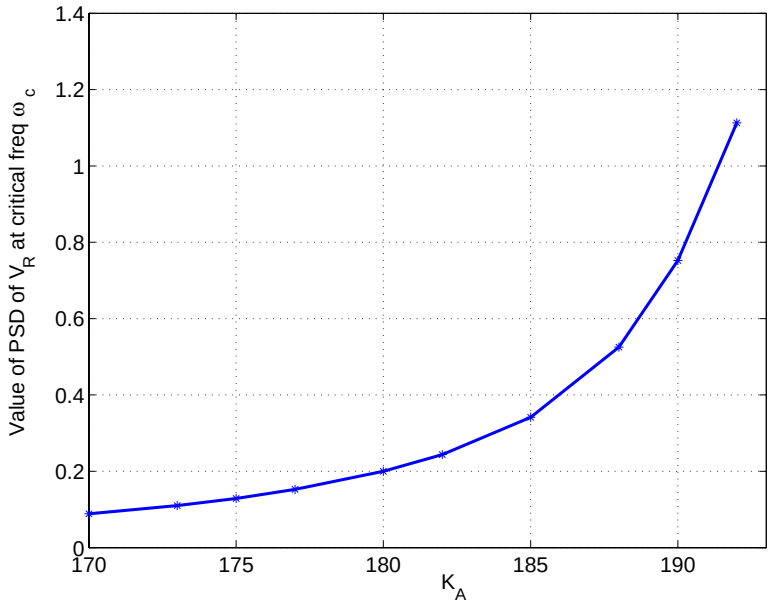

Figure 1.6. Variation of the peak value of the power spectral density of V_R as a function of the bifurcation parameter K_A. White Gaussian noise of zero mean and $(0.000032)^2$ power was added to P_m.

Table 1.3. Input-to-state participation factors for the 3-machine nine-bus system (partial listing). The load at bus 5 is 4.4 pu.

Input noise added to	States measured					
	E_{fd_1}	E_{fd_2}	E_{fd_3}	ω_1	ω_2	ω_3
P_{m_1}	3.0017	2.6973	2.1357	0.0033	0.0028	0.0031
P_{m_2}	2.6113	2.3465	1.858	0.0029	0.0024	0.0027
P_{m_3}	4.7816	4.2967	3.4022	0.0052	0.0044	0.0049
V_{ref_1}	0.0155	0.014	0.0111	0.0000169	0.0000143	0.000016
V_{ref_2}	0.0233	0.021	0.0166	0.0000255	0.0000215	0.00002409
V_{ref_3}	0.0475	0.0427	0.0338	0.0000519	0.000043	0.000049

peaks at 0.28 Hz and 1.3 Hz. These two frequencies correspond to the complex eigenvalues $\lambda_{3,4}$ and $\lambda_{1,2}$, respectively. Note that the peak at 1.3 Hz that corresponds to the pair of complex eigenvalues $\lambda_{1,2}$ is higher than the peak at 0.28 Hz. However, when the load at bus 5 is increased to 4.4 pu, the peak at 0.28 Hz becomes much larger than the one at 1.3 Hz (see Figure 1.8), which is an indicator that an instability is being approached. Figure 1.9 shows the power spectral density of E_{fd_1} for three values of P_{L_5}: 4.0 pu, 4.25 pu and 4.4 pu.

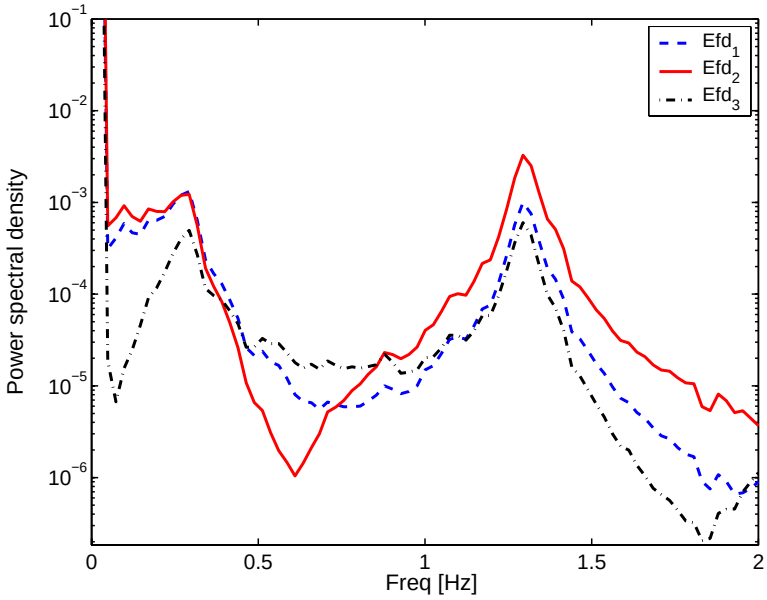

Figure 1.7. Power spectral densities of the states E_{fd_1}, E_{fd_2} and E_{fd_3}. The load on bus 5 was used as a bifurcation parameter. The load value is 4.0 pu. White Gaussian noise of zero mean and 0.05 power was added to P_{m_3}, the mechanical power of generator number 3.

5. Conclusions and suggested future research

An instability monitoring technique that aims at detection of impending instability has been described and illustrated in several example systems. The theme of the approach is to provide a warning when the margin of stability of a power system is compromised, without dependence on availability of an accurate system model. The approach consists of using additive white Gaussian noise probe signals and monitoring the spectral densities of certain measured states. Models are used in the approach in the selection of sites for probe signal injection and monitored output signal measurement (akin to actuator and sensor placement in control design). Input-to-state participation factors were presented and used as a tool for selection of probe and measurement siting.

The methods presented here are mathematically based but address engineering problems that are not easily defined in a crisp form. There are several directions that can be pursued for furthering the aims of this chapter.

A particularly challenging problem involves detection not only of the fact that an instability is near, but also detecting the severity of the

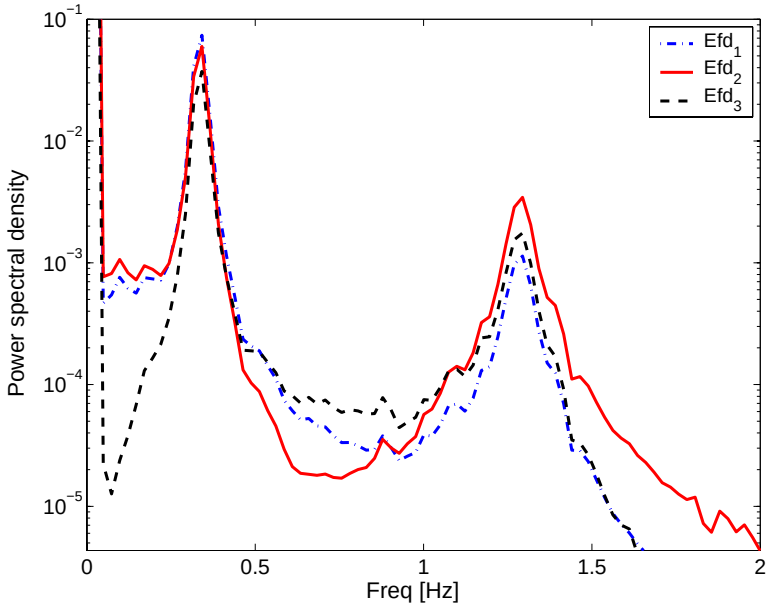

Figure 1.8. Power spectral densities of the states E_{fd_1}, E_{fd_2} and E_{fd_3}. The load on bus 5 was used as a bifurcation parameter. The load value is 4.4 pu. White Gaussian noise of zero mean and 0.05 power was added to P_{m_3}, the mechanical power of generator number 3.

impending instability from the point of view of nonlinear system behavior. For example, an oscillatory instability can be of the hunting type, in which small amplitude oscillations occur, or it can be divergent, resulting in complete loss of operation. Although this can be determined using analytical models using known methods of bifurcation analysis, it is not known how this can be achieved using a signal-based approach.

Another direction involves studying use of other probe signals in addition to AWGN. Examples include periodic signals, chaotic signals covering an appropriate frequency range, and colored noise signals. The relative advantages and disadvantages of the various probe signals should be considered. In this regard, connections to past work in real-time probing of power systems and aircraft dynamics should be studied. In research aircraft, for example, it is common to use "chirp" signals to probe the aircraft for its stability properties in various parts of its flight envelope.

The integration of stability monitoring and fault detection is an important long-term research goal. In the meantime, it will be useful to pursue case studies that will shed light on what will be required to achieve this integration.

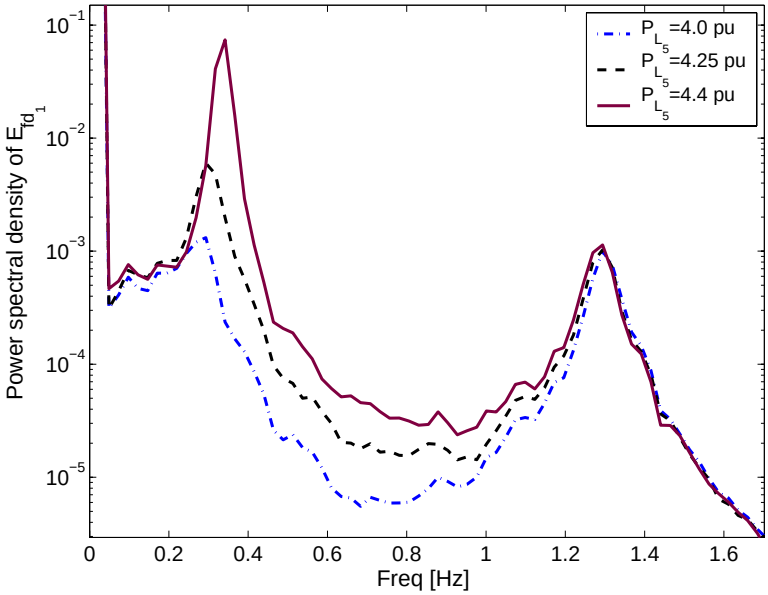

Figure 1.9. Power spectral density of E_{fd_1} for three values of P_{L_5} (the load on bus 5): $P_{L_5} = 4.0$ pu (dash-dotted line), $P_{L_5} = 4.25$ pu (dashed line) and $P_{L_5} = 4.4$ pu (solid line). White Gaussian noise of zero mean and 0.05 power was added to P_{m_3}, the mechanical power of generator number 3.

Finally, we mention the application of closed-loop monitoring systems to electric power system models. These designs, as described in [7], may provide added flexibility and surety to the conclusions reached regarding the presence of impending instability.

Acknowledgments

This research was supported in part by the National Science Foundation under Grants ECS-01-15160 and ANI-02-19162.

Appendix: Parameter values for the generators in Secs. 4.1 and 4.2

Parameters for the single generator model with dynamic load:

$M = 0.01464$, $C = 3.5$, $E_m = 1.05$, $Y_0 = 3.33$, $\theta_0 = 0$, $\theta_m = 0$, $K_{p\omega} = 0.4$, $K_{pv} = 0.3$, $K_{q\omega} = -0.03$, $K_{qv} = -2.8$, $K_{qv2} = 2.1$, $T = 8.5$, $P_0 = 0.6$, $P_1 = 0.0$, $Q_0 = 1.3$, $E_0 = 1.0$, $Y_m = 5.0$, $P_m = 1.0$, $d_m = 0.05$.

All values are in per unit except for angles, which are in degrees.

Parameters for the single generator model with an infinite bus:

The parameter values are given in Table 1.A.1 below.

Table 1.A.1. Parameter values for the single generator connected to an infinite bus model.

Synchronous machine	Exciter	Transmission line
$H = 2.37$ s	$K_E = -0.05$	$R_l^0 = 0.02$
$D = 1$ pu	$K_F = 0.02$	$X_l^0 = 0.40$
$X_d = 1.7$	$\tau_E = 0.50$ s	$R_l = \lambda R_l^0$
$X'_d = 0.245$	$\tau_F = 0.60$ s	$X_l = \lambda X_l^0$
$X_q = 1.64$	$\tau_A = 0.10$ s	
$\omega_0 = 377.0$ rad/s	$A_{EX} = 0.09$	
$\tau'_{d0} = 5.9$ s	$B_{EX} = 0.50$	

Notes

1. In [2], a new approach to defining modal participation factors was presented. The new approach involved taking an average or a probabilistic expectation of a quantitative measure of relative modal participation over an uncertain initial state vector. The new definitions were shown to reduce to the original definition of participation factors of [9, 12] if the initial state obeys a symmetry condition.

References

[1] E. H. Abed and P. P. Varaiya, "Nonlinear oscillations in power systems," *International J. Electrical Power and Energy Systems*, Vol. 6, No. 1, pp. 37–43, Jan. 1984.

[2] E. H. Abed, D. Linslay and W. A. Hashlamoun, "On participation factors for linear systems," *Automatica*, Vol. 36, No. 10, pp. 1489–1496, Oct. 2000.

[3] F. Milano "Power System Analysis Toolbox Documentation for PSAT," version 1.3.0, 2004 (available online at http://www.power.uwaterloo.ca/˜fmilano/).

[4] M. A. Hassouneh, H. Yaghoobi and E. H. Abed, "Monitoring and control of bifurcations using probe signals," in *Dynamics, Bifurcations and Control*, Lecture Notes in Control and Information Sciences, Vol. 273, F. Colonius and L. Gruene, Eds., Berlin: Springer Verlag, pp. 51–65, 2002.

[5] J. F. Hauer and M. J. Beshir, "Dynamic performance validation in the western power system," *Association of Power Exchanges*, Kananaskis, Alberta, Oct. 2000.

[6] C. W. Helstrom, *Probability and Stochastic Processes for Engineers*, Second Edition, Macmillan, 1991.

[7] T. Kim and E. H. Abed, "Closed-loop monitoring systems for detecting impending instability," *IEEE Trans. Circuits and Systems–I: Fundamental Theory and Applications*, Vol. 47, No. 10, pp. 1479–1493, Oct. 2000.

[8] F. L. Pagola, I. J. Perez-Arriaga, and G. C. Verghese, "On sensitivities, residues and participations: Applications to oscillatory stability analysis and control," *IEEE Transactions on Power Systems*, vol. 4, no. 1, pp. 278–285, Feb. 1989.

[9] I. J. Perez-Arriaga, G. C. Verghese, and F. C. Schweppe, "Selective modal analysis with applications to electric power systems, Part I: Heuristic introduction," *IEEE Trans. Power Apparatus and Systems*, Vol. 101, No. 9, pp. 3117–3125, Sep. 1982.

[10] P. W. Sauer and M. P. Pai, *Power System Dynamics and Stability*, Prentice Hall, New Jersey, 1998.

[11] T. Van Cutsem, "Voltage instability: Phenomena, countermeasures, and analysis methods," *Proc. IEEE*, Vol. 88, pp. 208–227, Feb. 2000.

[12] G. C. Verghese, I. J. Perez-Arriaga and F. C. Schweppe, "Selective modal analysis with applications to electric power systems, Part II: The dynamic stability problem," *IEEE Trans. Power Apparatus and Systems*, Vol. 101, No. 9, pp. 3126–3134, Sep. 1982.

[13] H. O. Wang, E. H. Abed and A.M.A. Hamdan, "Bifurcation, chaos, and crises in voltage collapse of a model power system," *IEEE Transactions on Circuits and Systems-I*, Vol. 41, No. 3, pp. 294–302.

[14] K. Wiesenfeld, "Noisy precursors of nonlinear instabilities," *Journal of Statistical Physics*, Vol. 38, no. 5-6, pp. 1071–1097, 1985.

[15] K. Wiesenfeld, "Virtual Hopf phenomenon: A new precursor of period doubling bifurcations," *Physical Review A*, Vol. 32, Sep. 1985.

[16] H. Yaghoobi and E. H. Abed, "Optimal actuator and sensor placement for modal and stability monitoring," *Proceedings of the American Control Conference*, pp. 3702–3707, San Diego, CA, June 1999.